Progress In Electromagnetics Research Letters, Vol. 56, 25–30, 2015

A Dumbbell-Shaped Dual-Band Metamaterial Antenna Using FDTD Technique

Sameer K. Sharma, Devvrat Gupta, Jai D. Mulchandani, and Raghvendra K. Chaudhary*

Abstract—In this study, a dumbbell-shaped metamaterial (MTM) antenna has been proposed for dual-band applications using finite difference time domain (FDTD) technique. Such a composite MTM antenna consists of dumbbell-shaped patch, microstrip and partial ground plane. The proposed antenna shows dual-band behavior having impedance bandwidths ($|S_{11}| < -10\,\text{dB}$) of 28.5% and 8.7% at 1.72 GHz and 3 GHz respectively. It has been designed to operate at various cellular standards such as GPS, GSM1800 and WCDMA. Design and analysis have been carried out using FDTD code based on uniform meshing and convolutional perfectly matched layer (CPML) absorbing boundary conditions. Further, simulation results have been verified using HFSS, and a prototype has been fabricated to validate the results experimentally. The overall electrical size of the proposed antenna is $0.287\lambda_o \times 0.346\lambda_o \times 0.009\lambda_o$. The proposed dual-band antenna offers excellent radiation characteristics with a gain of 1.2 dBi and 1.5 dBi at 1.72 GHz and 3 GHz respectively with omnidirectional radiation patterns in xz-plane.

1. INTRODUCTION

Recent advancements in wireless technology have pushed RF engineers to design smart antennas which could operate at various frequencies simultaneously in order to support different wireless standards. Planar microstrip technology has been extensively used as far as antenna design is concerned. These antennas are extremely cheap and provide higher levels of integration, ease of fabrication and low profile. Different slots, such as L-slot, C-slot, etc., can be introduced along with shortening pins and different resonating elements to realize multi-band operation [1, 2]. However, these antennas fail to provide desired levels of compactness which is extremely important for mobile units. In addition, they may also suffer from low or negative gain and irregular radiation patterns [3]. MTM antennas, on the other hand, support high levels of miniaturization as they support negative and zeroth order modes which are absent in traditional microstrip antennas. A lot of research work in this regard is available in literature [4–8], but these designs suffer from narrow bandwidths which restricts the data rate. Ha et al. [9] proposed a wideband antenna by loading a planar metamaterial unit cell but it failed in desired miniaturization as electrical size of proposed antenna was quite large. Based on similar design approach, Gupta et al. [10] proposed a compact zeroth order resonant (ZOR) antenna by loading a rectangular complimentary split ring resonator (CSRR) which provides handsome miniaturization but its operation is greatly restricted due to narrow bandwidth. Hence, there is a trade-off between bandwidth and antenna size. Hwang et al. [11] have designed an antenna for mobile handsets, but it offers negative gain and is quite large in size.

In this paper, FDTD technique has been used to design and analyze a dual-band metamaterial antenna which provides large bandwidth and compact size. It is designed to operate at various wireless

Received 1 July 2015, Accepted 30 August 2015, Scheduled 31 August 2015

* Corresponding author: Raghvendra Kumar Chaudhary (raghvendra.chaudhary@gmail.com).
The authors are with the Department of Electronics Engineering, Indian School of Mines Dhanbad, Dhanbad-826004, India.

standards such as GPS, GSM 1800 and WCDMA, respectively. The proposed MTM antenna consists of dumbbell-shaped patch, microstrip feed and partial ground plane. The upper patch behaves as a short circuit stub which virtually connects the thin shaft with ground plane. Partial ground plane improves input reflection coefficient by minimizing the back reflections.

2. ANTENNA GEOMETRY

The proposed antenna has been designed on an FR4 epoxy substrate ($\varepsilon_r = 4.4$, $\tan\delta = 0.02$) with thickness 1.6 mm and is shown in Fig. 1. The top consists of a dumbbell-shaped patch fed through microstrip feed. The lower patch generates a shunt capacitance due to abrupt transition from narrower feed and thin shaft which connects to upper patch. This thin shaft is virtually grounded by upper patch which acts like a short circuiting stub. Parametric analysis has been carried out in order to obtain optimized design dimensions of proposed antenna which are listed with Fig. 1.

Microstrip feed and lower patch acts as series inductance L_R while thin shaft is virtually grounded due to short circuited upper patch which behaves as shunt inductance L_L. The inductance offered by the upper patch is quite feeble and does not contribute much in resonant frequencies. The transitions between feed, lower patch and thin shaft results in parasitic shunt capacitance C_{R1}. Another shunt capacitance C_{R2} is realized between microstrip feed and ground plane. Equivalent circuit model so obtained is based on epsilon-negative (ENG) transmission line [12] approach and is shown in Fig. 2.

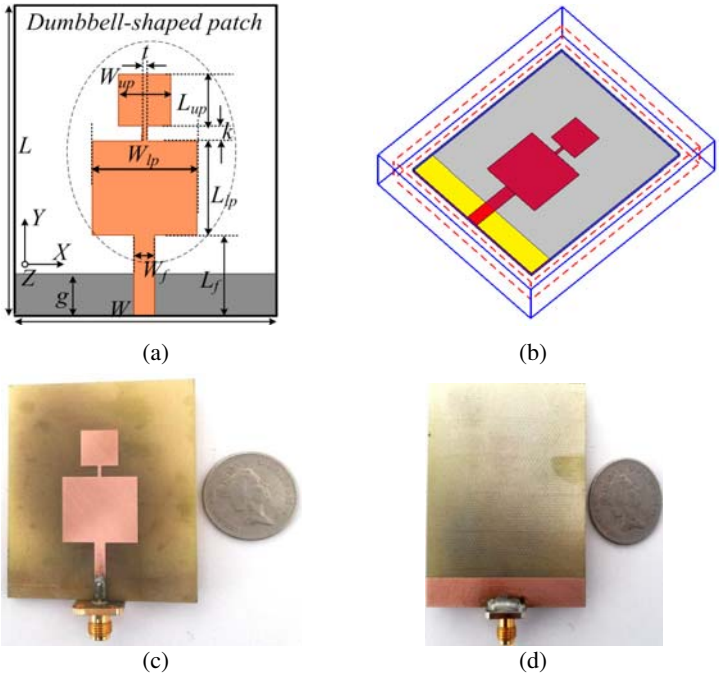

Figure 1. Geometry of proposed dumbbell-shaped metamaterial antenna [All dimensions are in mm: $L = 60$, $W = 50$, $g = 8$, $W_f = 4$, $L_f = 15.6$, $L_{lp} = 18.1$, $L_{up} = 10$, $W_{lp} = 20$, $W_{up} = 10$, $t = 1$, $k = 2.9$]. (a) 2-D view. (b) Designed antenna using FDTD code. (c) Top-view of fabricated antenna. (d) Bottom-view of fabricated antenna.

3. FDTD THEORY

Time-dependent Maxwell equations can be easily solved using FDTD which is based on ordinary partial differential equations. The structure is designed and solved using Yee's leapfrog arrangement in where each electric field vector is surrounded by four magnetic field vector, and each magnetic field vector is surrounded by four electric field vectors [13]. The structure is decomposed into numerous Yee cells

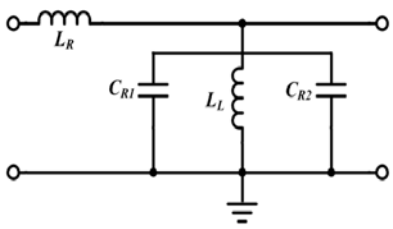

Figure 2. Equivalent circuit model of proposed metamaterial antenna using ENG transmission line.

and then solved independently to obtain electric and magnetic fields. These equations so obtained are updated regularly after every time step Δt which controls the simulation time.

The spatial increments in x, y and z directions restrict the numerical dispersion under specified limit while controlling the simulation time and memory space. The relation between spatial increments and time step is given by Equation (1). With increase in spatial dimensions (coarse meshing), computational time can be significantly decreased at the cost of accuracy. However, fine sampling results in increased memory space and time for better accuracy. Hence, there is a trade-off between stability and time complexity which is referred as CFL stability limit.

The updating equations of electric and magnetic fields are based on central difference and are given by Equations (2), (3), (4) and (5) respectively [14].

$$\Delta t \leq \frac{1}{c\sqrt{\left(\frac{1}{\Delta x}\right)^2+\left(\frac{1}{\Delta y}\right)^2+\left(\frac{1}{\Delta z}\right)^2}} \tag{1}$$

$$\frac{\partial E_x}{\partial t} = \frac{1}{\varepsilon_x}\left(\frac{\partial H_z}{\partial y} - \frac{\partial H_y}{\partial z} - \sigma_x^e E_z - j_{ix}\right) \tag{2}$$

$$\frac{E_x^{n+1}(i,j,k) - E_x^n(i,j,k)}{\Delta t} = \frac{1}{\varepsilon_x(i,j,k)}\frac{H_z^{n+\frac{1}{2}}(i,j,k) - H_z^{n+\frac{1}{2}}(i,j-1,k)}{\Delta y}$$
$$-\frac{1}{\varepsilon_x(i,j,k)}\frac{H_y^{n+\frac{1}{2}}(i,j,k) - H_y^{n+\frac{1}{2}}(i,j,k-1)}{\Delta z} - \frac{\sigma_x^e(i,j,k)}{\varepsilon_x(i,j,k)}E_x^{n+\frac{1}{2}}(i,j,k) - \frac{1}{\varepsilon_x(i,j,k)}j_{ix}^{n+\frac{1}{2}}(i,j,k) \tag{3}$$

$$\frac{\partial \mathrm{H_X}}{\partial \mathrm{t}} = \frac{1}{\mu_x}\left(\frac{\partial E_y}{\partial z} - \frac{\partial E_z}{\partial y} - \sigma_x^m H_x - M_{ix}\right) \tag{4}$$

$$\frac{\mathrm{H}_x^{n+\frac{1}{2}}(i.j.k) - \mathrm{H}_x^{n-\frac{1}{2}}(i.j.k)}{\Delta \mathrm{t}} = \frac{1}{\mu_x(i.j,k)}\frac{E_y^n(i,j,k+1) - E_y^n(i,j,k)}{\Delta z}$$
$$-\frac{1}{\mu_x(i.j,k)}\frac{E_z^n(i,j+1,k) - E_z^n(i,j,k)}{\Delta y} - \frac{\sigma_x^m(i,j,k)}{\mu_x(i.j,k)}H_x^n(i,j,k) - \frac{1}{\mu_x(i.j,k)}M_{ix}^n(i,j,k) \tag{5}$$

Elsherbeni and Demir [14] have proposed a FDTD code which has been modified to model and analyze the proposed dual-band metamaterial antenna. The simple geometry of the proposed antenna allows easy modeling as meshing is uniform and orthogonal. CPML based absorbing boundary conditions is highly effective in absorbing decaying EM waves which results in fast computation and low storage requirement. Huygens surface equivalence theorem has been implemented at the output boundary to obtain near-to-far field transformation [14].

4. RESULTS & DISCUSSIONS

Figure 3 shows the variation of input reflection coefficient with increase in length of ground plane (g). It is seen that with increase in g, impedance matching at 3 GHz decreases significantly. However, there is no effect on input reflection coefficient of first band. Variation of input reflection coefficient with increase in width of microstrip feed (W_f) is shown in Fig. 4. The width of microstrip feed is optimized

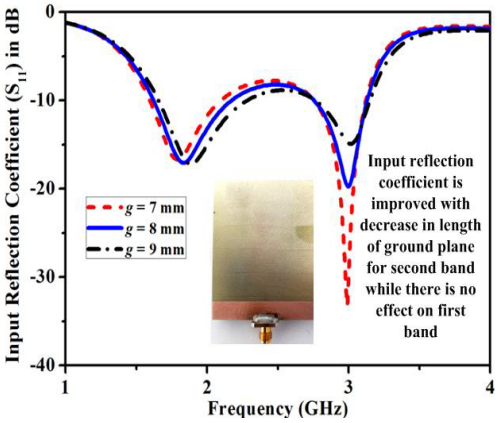

Figure 3. Variation in input reflection coefficient of proposed antenna with change in length of ground plane.

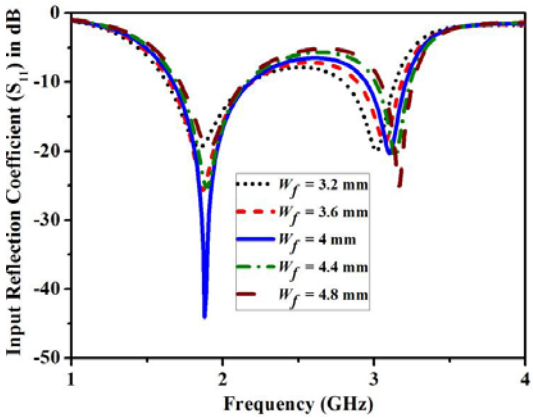

Figure 4. Variation in input reflection coefficient of proposed antenna with change in width of micro feed.

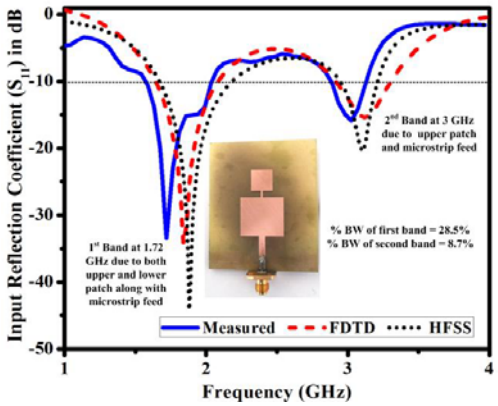

Figure 5. Measured and simulated input reflection coefficient of proposed metamaterial antenna.

Table 1. Performance of proposed antenna at various wireless standards.

Standard	Frequency (GHz)	Measured Gain (dBi)	Radiation Efficiency (%)
GPS	1.575 GHz	0.9 dBi	96.4%
GSM 1800	1.8 GHz	1.2 dBi	92.3%
WCDMA	1.9 GHz	1.23 dBi	90.1%

for the best impedance matching at 1.72 GHz while impedance matching remains unaffected for the second band.

The proposed antenna exhibits dual-band behavior with first band resonant at 1.72 GHz and second band at 3 GHz having impedance bandwidth of 28.5% and 8.7%, respectively. Fig. 5 illustrates the input reflection coefficient of the proposed dumbbell-shaped metamaterial antenna. It has been designed to operate at various wireless standards such as GPS, GSM1800 and WCDMA. Measurement results matches well with the simulation results. Table 1 shows the performance of proposed antenna at these standards state above.

Radiation patterns of the proposed antenna are shown in Fig. 6. The proposed MTM antenna exhibits omnidirectional radiation patterns in xz-plane and dipolar-type in yz-plane at both 1.72 GHz

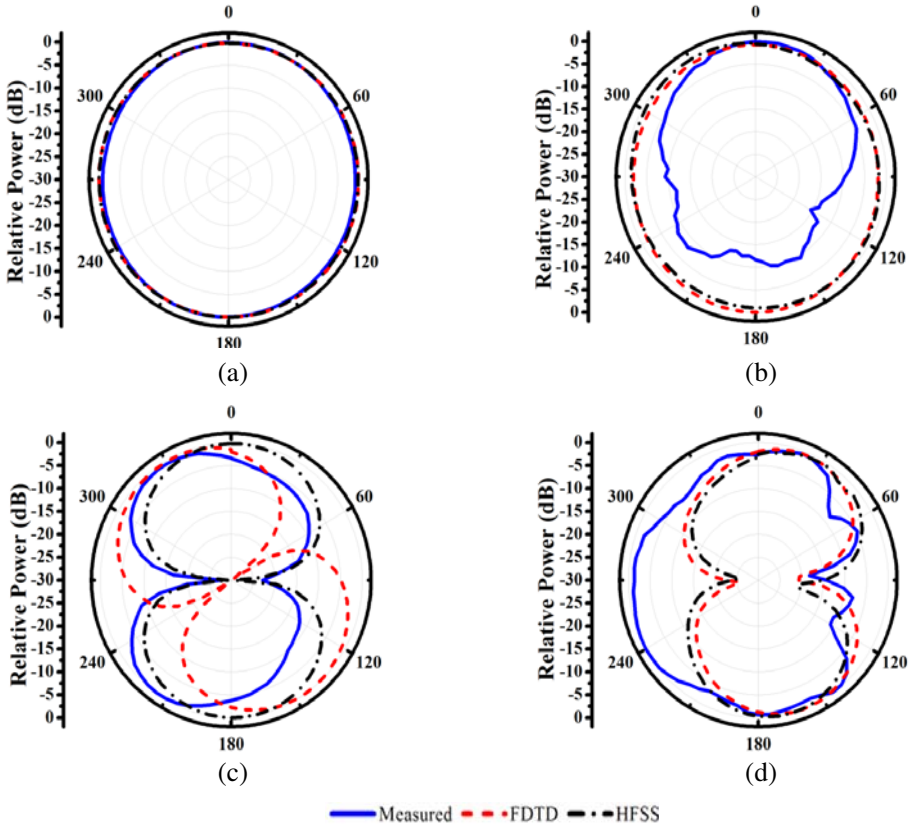

Figure 6. Radiation patterns of proposed dual-band metamaterial antenna. (a) xz-plane at 1.72 GHz. (b) xz-plane at 3 GHz. (c) yz-plane at 1.72 GHz. (d) yz-plane at 3 GHz.

Table 2. Comparison of proposed antenna with earlier reported antennas.

	Electrical size in terms of λ_o	Percentage Bandwidth	Gain (dBi)
Proposed work	$0.287\lambda_o \times 0.346\lambda_o \times 0.009\lambda_o$	28.5%, 8.7%	1.2 dBi, 1.5 dBi
[9]	$0.505\lambda_o \times 0.442\lambda_o \times 0.02\lambda_o$	6.8%	3.85 dBi
[10]	$0.321\lambda_o \times 0.285\lambda_o \times 0.011\lambda_o$	5.3%	2.6 dBi
[15]	$0.35\lambda_o \times 0.35\lambda_o \times 0.013\lambda_o$	12.4%	<0 dBi

and 3 GHz with very low cross-polarization levels. Measurement results appear to be distorted as compared with simulation results. It is because ground plane is partial which causes high amount of current to flow through which thereby loads the coaxial cable. This current loading in the coaxial cable results in partial distortion of radiation patterns. The proposed MTM antenna offers a gain of 1.2 dBi at 1.72 GHz and 1.5 dBi at 3 GHz with a simulated radiation efficiency of 91.5% and 83.9% respectively. Table 2 shows the comparison of proposed antenna with earlier reported work.

5. CONCLUSION

Design and analysis of dumbbell-shaped metamaterial antenna has been discussed for mobile applications using FDTD techniques. The proposed antenna is designed to operate at GPS, GSM 1800 and WCDMA and offer dual-band response with resonant frequencies of 1.72 GHz and 3 GHz. An equivalent circuit model based on ENG transmission line has also been proposed. The overall electrical

size of antenna is $0.287\lambda_o \times 0.346\lambda_o \times 0.009\lambda_o$ and offers an impedance bandwidth of 28.5% and 8.7% respectively for first and second band respectively. It offers a gain of 1.2 dBi and 1.5 dBi at 1.72 GHz and 3 GHz with excellent radiation characteristics which makes it suitable for use in mobile applications.

ACKNOWLEDGMENT

Authors would like to thank Dr. K. V. Srivastava, Associate Professor, IIT Kanpur, India for providing lab facility to measure S-parameters and radiation patterns of fabricated prototype.

REFERENCES

1. Wong, K. L. and H. B. Hsieh, "Dual-frequency circular microstrip antenna with a pair of arc-shaped slots," *Microw. Opt. Technology Lett.*, Vol. 19, 410–412, 1998.
2. Waterhouse, R. B., S. D. Targonski, and D. M. Kokotoff, "Design and performance of small printed antennas," *IEEE Trans. Antenna Propag.*, Vol. 46, 1629–1633, 1998.
3. Waterhouse, R. B., *Printed Antennas for Wireless Communication*, Wiley-IEEE Press, New York, 2007.
4. Caloz, C. and T. Itoh, *Electromagnetic Metamaterials: Transmission Line Theory and Microwave Applications*, Wiley-IEEE Press, New York, 2005.
5. Sharma, S. K. and R. K. Chaudhary, "Dual-band metamaterial-inspired antenna for mobile applications," *Microw. Opt. Technology Lett.*, Vol. 57, 1444–1447, 2015.
6. Niu, B. J. and Q. Fang, "Bandwidth enhancement of CPW-fed antenna based on epsilon negativezeroth and first-order resonators," *IEEE Antennas and Wireless Propag. Lett.*, Vol. 12, 1125–1128, 2013.
7. Sharma, S. K., A. Gupta, and R. K. Chaudhary, "Compact CPW-fed CHSSR antenna for WLAN," *IEEE MTT Int. Microw. and RF Conference (IMaRC)*, 114–117, Bangalore, India, 2014.
8. Kim, T. G. and B. Lee, "Metamaterial based compact zeroth order resonant antenna," *Electronics Lett.*, Vol. 45, 12–13, 2009.
9. Ha, J., K. Kwon, Y. Lee, and J. Choi, "Hybrid mode wideband patch antenna loaded with a planar metamaterial unit cell," *IEEE Trans. Antennas and Propag.*, Vol. 60, 1143–1147, 2012.
10. Gupta, A., S. K. Sharma, and R. K. Chaudhary, "A compact dual-mode metamaterial-inspired antenna using rectangular-type CSRR," *Progress In Electromagnetics Research C*, Vol. 57, 35–42, 2015.
11. Hwang, S. H., T. S. Yang, J. H. Byun, and A. S. Kim, "Design and analysis of metamaterial antenna for mobile handset application," *3rd European Conference on Antennas and Propag.*, 3563–3566, Berlin, Germany, 2009.
12. Park, J. H., Y. H. Ryu, J. G. Lee, and J. H. Lee, "Epsilon negative zeroth order resonating antenna," *IEEE Trans. Antennas and Propag.*, Vol. 55, 3710–3712, 2007.
13. Yee, K., "Numerical solution of initial boundary value problems involving Maxwell's equations in isotropic media," *IEEE Trans. Antennas and Propag.*, Vol. 14, 302–307, 1966.
14. Elsherbeni, A. Z. and V. Demir, *The Finite-difference Time-domain Method for Electromagnetics with MATLAB Simulations*, SciTech Pub., Norwood, MA, 2009.
15. Majedi, M. S. and A. R. Attari, "A compact and broadband metamaterial-inspired antenna," *IEEE Antennas and Wireless Propag. Lett.*, Vol. 12, 345–348, 2013.